ACS OMEGA

http://pubs.acs.org/journal/acsodf

Article

Sensitivity Analysis of a Bench-Scale Pyrolysis Model for Composite Materials: A Case Study of Poly(lactic acid)/Melamine/Ammonium Polyphosphate

Zeyue Shen, Yue Qiu, Weichen Song, and Qi Sun*

Cite This: *ACS Omega* 2022, 7, 19648−19664

Read Online

ACCESS | Metrics & More | Article Recommendations

ABSTRACT: On the basis of a well-developed bench-scale pyrolysis model that relates material composition to flammability, this paper applied mathematical simulations to explore the model sensitivity for the prediction of fire behavior of composite materials. A pyrolysis model for poly(lactic acid) blended with melamine and ammonium polyphosphate as the reference material was selected as the case for analysis. The model input parameters for simulations include the heat of reaction, apparent activation energy, and pre-exponential factor of 15 reactions, as well as the thermal conductivity, emissivity coefficient, absorption coefficient, and density of 17 condensed-phase components. Each reaction-related or component-related parameter was adjusted from 80% of the model value to 120% with a 5% or 10% gradient. Finally, 826 simulation cases in total were calculated for analysis. Both the mass loss rate and the heat release rate of each case were calculated to characterize the sensitivity, which showed the same pattern. Finally, seven primary reactions and five key condensed-phase components with high sensitivity were identified. The predicted fire behaviors are highly related to the kinetics of the reactions between virgin components or reactions where virgin components play an important role in, including the pyrolysis of melted poly(lactic acid), the first step in the pyrolysis of melamine, the first step in the pyrolysis of ammonium polyphosphate, the reaction between melted poly(lactic acid) and melamine, the reaction between ammonium polyphosphate and melamine, and further decomposition of the generated new condensed-phase component. Particularly, the activation energy of these reactions is of sensitivity larger than 5% or 15%. The heat of decomposition of pyrolysis of melted poly(lactic acid) also showed a sensitivity of 2%−5%. The pre-exponential factor of all reactions showed a sensitivity of less than 2%, which can be ignored. Inputting the proper density is important for the prediction of fire behavior as the sensitivity is larger than 2%. The sensitivity of the milligram-scale model was also processed and compared. These simulations provided a fundamental understanding of the sensitivity of thermophysical and chemical properties and thus provide advanced insights into fire behavior modeling and new composite material design.

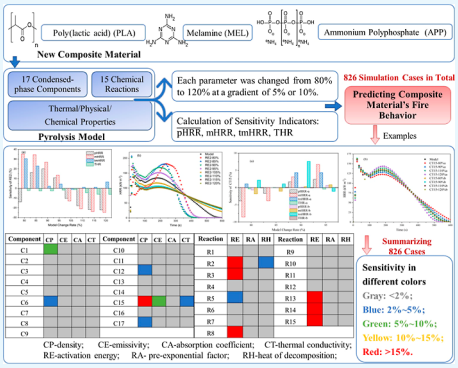

1. INTRODUCTION

The application of numerical tools in the study of flammability of composite materials has become general nowadays.[1] The tendency is also increasing with the development of the performance-based design of biodegradable composite materials as a sustainable alternative to traditional petroleum-based synthetic materials.[2] Despite the wide use of pyrolysis modeling approaches, they still cannot accurately predict the fire behavior of composites.[3] Therefore, researchers started to explore how the uncertainty in input parameters contributes to the pyrolysis modeling results.[3,4] For example, Bal[4] conducted a series of uncertainty and complexity analyses in pyrolysis modeling using polymethyl methacrylate (PMMA) as a reference material and identified that the input value of some properties would highly influence the prediction of fire behavior, while some input parameters showed a limited effect.

In recent years, developing degradable plastics with low flammability has contributed to the availability of new environmental friendly composite materials for wider application scenarios.[5] Compared to PMMA, the pyrolysis modeling of these flame-retardant materials is more complex but necessary for material design. Limited discussions have been made on the uncertainty and sensitivity of the corresponding pyrolysis models. For example, poly(lactic acid) (PLA) is a typical biodegradable thermoplastic polyester with a wide region of application areas, including tissue engineering, packaging, biomedical, and so on.[6,7] Two halogen-free flame-retardant additives, ammonium polyphosphate (APP) and

Received: March 8, 2022
Accepted: May 19, 2022
Published: May 31, 2022

melamine (MEL), have been added to PLA to overcome its major disadvantage of high flammability.[8]

To analyze the relationships between material composition, thermophysical properties, and fire behavior, previous researchers have conducted both experiments and simulations regarding the composite system of PLA/MEL/APP to predict the pyrolysis behavior.[7,9−11] A one-dimensional pyrolysis model for PLA/MEL/APP has been developed and verified by both milligram-scale[11] and bench-scale experiments.[10] The model showed the capability to predict the flammability of the composite material under different fire scenarios with acceptable errors. However, questions were proposed regarding the sensitivity of this model for predicting the fire behavior of the composite material, which will be discussed in the current study.

According to previous studies,[10,11] the fundamental input data of the fully developed pyrolysis model for PLA/MEL/APP involve 15 sets of reactions, as well as the kinetics, thermodynamics, and thermophysical properties of 17 components, which determine the burning rates of the pyrolyzing solids under different compositions. Although the importance of accuracy of these inputs has been widely recognized,[12−14] limited discussions have been made about how uncertainties of these inputs influence the pyrolysis modeling results, mainly the heat release rate (HRR). Note that HRR is arguably the most critical parameter that defines the materials' fire hazard,[15] indicating how much a given material contributes to the energy production and fire growth.

All pyrolysis modeling has unavoidable deviations from the real HRR. Sensitivity analysis of the developed pyrolysis models not only indicates the priorities of components for composition design, but also provides practical insights into fire safety-related decisions.[16,17] For example, material designers may require information about the effects of certain components on thermal or mechanical properties to develop composites that satisfy certain thermal or mechanical needs; fire safety researchers will refer to the errors of some key parameters, such as thermal conductivity for the prediction of fire behavior. To meet these needs, the role of each parameter in the pyrolysis model should be determined. Most pyrolysis model studies focus on the establishment of complex models, but not all reactions or components are equally important to the prediction results of pyrolysis behavior.

Therefore, a series of sensitivity analyses are conducted in this study to explore how the uncertainties of different parameters affect the pyrolysis simulation results using PLA/MEL/APP as the reference material. According to the proposed pyrolysis model,[10,11] the uncertainties mainly come from the reaction kinetics (mainly activation energy and pre-exponential factor), thermodynamics (heat of reaction), and a series of thermophysical properties (thermal conductivity, density, emissivity, and absorption coefficient) of condensed-phase components. Relevant analyses are performed by focusing on a particular system involving 5 wt % MEL and 25 wt % APP (noted as PLA70MEL5APP25). A composite material in this composition was selected because, compared to the blends with other compositions, this reference material had been proved by bench-scale pyrolysis experiments to have an outstanding flame-retardant effect as well as good mechanical property, and it had the potential to be widely used as a new flame-retardant composite.

On the basis of 826 calculation cases in total, the sensitivity of each parameter was studied by adjusting from 80% of the model value to 120% with a 5% or 10% gradient. This study has two highlights. On the one hand, it explores the sensitivity of the whole pyrolysis model by analyzing how the adjustment of each parameter could influence the predicted fire behavior; on the other hand, it identifies the major reactions and components that play a vital role in the prediction of fire behavior of the material to simplify the application of pyrolysis model. Findings of this paper are expected to assist with material design and fire behavior simulations in the relevant fields.

2. METHODOLOGY

2.1. Brief of the Model. Sensitivity analysis was conducted using a generalized pyrolysis modeling tool by adjusting the inputs of a previously developed pyrolysis model for PLA/MEL/APP. The summary of the model is presented in Tables 1−3. Tables 1 and 2 present the semi-global decomposition mechanism of PLA/MEL/APP, and the corresponding kinetics and thermodynamics of each reaction, respectively. Table 3 summarizes the values of thermophysical properties that control the heat and mass transfer in the condensed phase during pyrolysis. The model has been verified against both milligram-scale and bench-scale experiments.[10,11]

Table 1. Decomposition Mechanism of PLA/MEL/APP Blends for Sensitivity Analysis[a]

sub-model	#	reactions
PLA	R1	PLA → PLA_Melt
	R2	PLA_Melt → 0.02 PLA_Res + 0.98 PLA_G
MEL	R3	MEL → 0.82 MEL_Res + 0.18 MEL_G1
	R4	MEL_Res → MEL_G2
APP	R5	APP → 0.90 APP_Res1 + 0.10 APP_G1
	R6	APP_Res1 → 0.90 APP_Res2 + 0.10 APP_G2
	R7	APP_Res2 → 0.28 APP_Res3 + 0.72 APP_G3
PLA/MEL	R8	PLA_Melt + 0.28 MEL→ 0.42 PLA_MEL_Res1 + 0.86 PLA_MEL_G1
	R9	PLA_MEL_Res1 → 0.75 PLA_MEL_Res2 + 0.25 PLA_MEL_G2
	R10	PLA_MEL_Res2 → 0.80 PLA_MEL_Res3 + 0.20 PLA_MEL_G3
PLA/APP	R11	PLA_Melt + 0.21 APP → 1.10 PLA_APP_Res1 + 0.11 PLA_APP_G1
	R12	PLA_APP_Res1 → 0.22 PLA_APP_Res2 + 0.78 PLA_APP_G2
PLA/MEL/APP	R13	APP + 0.14 MEL → 1.14 APP_MEL_Res1
	R14	APP_MEL_Res1 → 0.45 APP_MEL_Res2 + 0.55 APP_MEL_G1
	R15	PLA_Melt + 0.06 APP_MEL_Res1 → 0.14 Res1 + 0.92 PLA_APP_MEL_G1

[a]Reprinted with permission from ref 11. Copyright 2016, *Polym. Degrad. Stabil.*

Comparisons between the experimental and modeling results of two PLA/MEL/APP blends under two radiant fluxes have been presented in the previous literature,[10] showing the good prediction performance of the model. The model was capable of predicting the mass loss rate (MLR). The simulated HRR was also consistent with the early experimental study by fire tests. Detailed information of the experimental and modeling methodology is summarized in these papers.[10,11] Please note that the current model obtained by inverse analysis of experiments was proved to be of the best fitting performance. As a case study, this study selects the composite of PLA70MEL5APP25 for sensitivity analysis by exposing the

https://doi.org/10.1021/acsomega.2c01402
ACS Omega 2022, 7, 19648−19664

Table 2. Kinetic and Thermodynamic Parameters of PLA/MEL/APP Blends for Sensitivity Analysis[a]

reaction #	A (s^{-2})	E (J mol^{-1})	h (J kg^{-1})	reaction #	A (s^{-2})	E (J mol^{-1})	h (J kg^{-1})
R1	6.0×10^{40}	3.57×10^{5}	5.20×10^{4}	R9	3.2×10^{17}	2.05×10^{5}	1.43×10^{5}
R2	2.1×10^{21}	2.85×10^{5}	1.02×10^{6}	R10	3.2×10^{16}	2.06×10^{5}	5.00×10^{4}
R3	1.0×10^{16}	1.98×10^{5}	1.90×10^{5}	R11	7.0×10^{11}	1.71×10^{5}	7.80×10^{4}
R4	5.0×10^{18}	2.40×10^{5}	9.94×10^{5}	R12	9.8×10^{10}	1.58×10^{5}	7.88×10^{5}
R5	6.0×10^{9}	1.40×10^{5}	8.80×10^{5}	R13	6.0×10^{40}	3.90×10^{5}	0
R6	1.0×10^{2}	6.30×10^{4}	5.80×10^{5}	R14	5.0×10^{3}	9.88×10^{4}	4.50×10^{5}
R7	6.0×10^{10}	2.23×10^{5}	6.80×10^{5}	R15	2.0×10^{5}	1.21×10^{5}	1.02×10^{6}
R8	6.0×10^{29}	3.63×10^{5}	5.51×10^{5}				

[a]Reprinted with permission from ref 11.Copyright 2016, *Polym. Degrad. Stabil.*

Table 3. Thermal−Physical Properties of Condensed-Phase Components for Sensitivity Analysis[a]

#	component	c (J kg^{-1} K^{-1})	ρ (kg m^{-3})	ε	κ (m^2 kg^{-1})	k (Wm^{-1} K^{-1})	λ (m^2 s^{-1})
C1	PLA	$100 + 3.70T$	1240	0.92	1.16	0.12	2×10^{-5}
C2	PLA_Melt	$1450 + 1.20T$	500	0.92	5	$0.12 + 0.0005T$	2×10^{-5}
C3	PLA_Res	1700	1240	0.94	100	$0.12 + 0.0005T$	2×10^{-5}
C4	MEL	$80 + 2.80T$	1570	0.92	4.4	$0.12 + 0.0005T$	2×10^{-5}
C5	MEL_Res	$890 + 1.40T$	72	0.94	100	$0.12 + 0.0005T$	2×10^{-5}
C6	APP	$740 + 1.76T$	1900	0.92	2.3	$0.12 + 0.0005T$	2×10^{-5}
C7	APP_Res1	$740 + 1.76T$	1282	0.93	34.9	$0.12 + 0.0005T$	2×10^{-5}
C8	APP_Res2	$2370 + 0.88T$	665	0.93	67.5	$0.12 + 0.0005T$	2×10^{-5}
C9	APP_Res3	4000	47	0.94	100	$0.12 + 0.0005T$	2×10^{-5}
C10	PLA_MEL_Res1	$-100 + 4.70T$	120	0.92	4.7	$0.3 + 0.002T$	2×10^{-5}
C11	PLA_MEL_Res2	$-100 + 4.70T$	90	0.93	52.35	$0.3 + 0.002T$	2×10^{-5}
C12	PLA_MEL_Res3	$-100 + 4.70T$	72	0.94	100	$0.03 + 0.0002T + 1 \times 10^{-9}T3$	2×10^{-5}
C13	PLA_APP_Res1	$910 + 2.60T$	214	0.92	3.65	$0.12 + 0.0005T$	2×10^{-5}
C14	PLA_APP_Res2	$910 + 2.60T$	47	0.94	100	$0.12 + 0.0005T$	2×10^{-5}
C15	APP_MEL_Res1	3000	104	0.92	3.35	$0.5 + 0.0001T$	2×10^{-8}
C16	APP_MEL_Res2	$910 + 2.60T$	47	0.94	100	$0.06+ 5 \times 10^{-10}T^3$	2×10^{-5}
C17	PLA_APP_MEL_Res1	$910 + 2.60T$	47	0.94	100	$0.06 + 5 \times 10^{-10}T^3$	2×10^{-8}

[a]Reprinted with permission from ref 10. Copyright 2020, *Composites, Part B.*

bench-scale material (with a thickness of 3 mm and a diameter of 7 cm) to a commonly used fire radiant flux of 65 kW m^{-2}.

It should be addressed that the chemical nature of Res and G of the reactions listed in Table 1 refers to components in the form of a residue (including intermediates and final residues) and a gas, respectively. The model assumes that each residue is of condensed phase and will either further decompose into gases or is in the form of char if the pyrolysis reaction is completed. The model only decides the thermal properties of condensed-phase components, while the generated gases are assumed to be fully released. Both MEL and APP act in the condensed phase by reacting with PLA to generate condensed-phase intermediates, which further decompose to generate more char. Besides, although the reference material for sensitivity analysis in this paper is PLA70MEL5APP25, the model shown in Tables 1−3 is also feasible for the PLA/MEL/APP blends with other material compositions.

2.2. Modeling Principle. The governing equations for modeling of this study are provided as eqs 1−7.[10,11]

$$\frac{\partial \xi_j}{\partial t} = \sum_{i=1}^{N_r} \theta_i^j r_i - \frac{\partial J_g}{\partial x} + \frac{\partial}{\partial x}\left(\xi_j \int_0^x \frac{1}{\rho}\frac{\partial \rho}{\partial t}\,dx\right) \quad (1)$$

$$\sum_{j=1}^{N} \xi_j c_j \frac{\partial T}{\partial t} = -\sum_{i=1}^{N_r} h_i r_i - \frac{\partial q_x}{\partial x} - \frac{\partial I_{ex}}{\partial x} + \frac{\partial I_{rr}}{\partial x} - \sum_{g=1}^{N_g} c_g J_g \frac{\partial T}{\partial x} + c\rho \frac{\partial T}{\partial x}\int_0^x \frac{1}{\rho}\frac{\partial \rho}{\partial t}\,dx \quad (2)$$

$$r_i = A_i \exp\left(-\frac{E_i}{R_u T}\right)\xi_{COMP1}\xi_{COMP2} \quad (3)$$

$$J_g = -\rho_g \lambda \frac{\partial(\xi_g/\rho_g)}{\partial x} \quad (4)$$

$$q = -k\frac{\partial T}{\partial x} \quad (5)$$

$$\frac{\partial I_{ex}}{\partial x} = -I_{ex}\sum_{j=1}^{N} \kappa_j \xi_j \quad (6)$$

$$\frac{\partial I_{rr}}{\partial x} = \frac{\varepsilon\sigma T^4}{I_{ex}^0}\frac{\partial I_{ex}}{\partial x} \quad (7)$$

Equation 1 provides the mass conservation for the j-th component in terms of the mass concentration of the component, ξ_j (kg m^{-3}). The mass conservation accounts for the consumption or production of the j-th component due to the chemical reactions occurring at a rate defined in eq 3 (in the absence of the second reactant, ξ_{COMP2} is set to be 1), mass

https://doi.org/10.1021/acsomega.2c01402
ACS Omega 2022, 7, 19648−19664

transport of gaseous products (labeled with the subscript g) within the condensed phase given by eq 4, and mass transport associated with contraction or expansion of the material with respect to a stationary boundary (x = 0, back sample surface). Equation 2 represents the energy conservation in terms of temperature, T (K). The energy conservation accounts for heat flow due to the thermal decomposition reactions and phase transitions and heat conduction within the condensed phase defined in eq 5. The energy conservation also accounts for the absorption of radiant heat from external sources defined in eq 6, radiant heat loss from the material to the environment defined in eq 7, convective heat transfer due to gas transport, and energy flow associated with contraction or expansion of the material with respect to the stationary boundary.

The symbols in eqs 1−7 are defined as follows: t (s) denotes the time; N_r, N, and N_g represent the total number of the reactions, components, and gaseous components, respectively; c (J kg^{-1} K^{-1}) is the heat capacity; k (W m^{-1} K^{-1}) is the thermal conductivity; and λ (m^2 s^{-1}) denotes the gas-transfer coefficient. Properties without subscripts are calculated by considering either the mass or volume fraction of each component in a mixture.[14] Subscripts i and j represent the i-th reaction and j-th component, respectively. θ_i^j is a stoichiometric mass coefficient, which is negative when component j is the i-th reaction's reactant and positive if it is a product component. h_i (J kg^{-1}) is the temperature-dependent heat released or absorbed in each chemical reaction or phase transition. A_i (s^{-1} for the first-order and m^3 kg^{-1} s^{-1} for the second-order reactions) is the Arrhenius pre-exponential factor for reaction i. E_i (J mol^{-1}) is the activation energy for reaction i. R_u (J mol^{-1} K^{-1}) is the universal gas constant. r_i (kg m^{-3} s^{-1}) is the reaction rate. J_g (kg m^{-2} s^{-1}) and q (W m^{-2}) denote the mass transport flux of gaseous products and heat conduction flux, respectively. I_{ex} (W m^{-2}) is the radiation flux absorbed by the sample (including in-depth) from the external sources. I_{rr} (W m^{-2}) is the radiant heat loss from material to the environment. The term I_{ex}^0 in eq 7 represents the net external radiative flux through the material boundary and σ (W m^{-2} K^{-4}) is the Stefan−Boltzmann constant. A more detailed explanation of these equations and their numerical solution methodology can be found in these earlier publications.[14,18]

Being consistent with bench-scale cone radiation heating experiments[10] and following the requirement of ASTM E1354,[19] the simulated pyrolysis scenario was used to expose the top surface of a one-dimensional material (with 3 mm thickness in a diameter of 7 cm) to a constant radiant heat flux of 65 kW m^{-2}. All calculations were conducted using Δx = 10^{-5} m spatial discretization and 0.005 s time step. Other boundary conditions were applied as mentioned in the previous study for pyrolysis model design.[10]

2.3. Overview of Sensitivity Analysis Methodology. The simulations of this study consist of three parts. The first part is to analyze how uncertainties in reaction kinetics influence the modeling results. This is conducted by changing the activation energy, pre-exponential factor, and heat capacity of each reaction one by one. Relevant results are presented in Section 3.1. The second part (Section 3.2) is to explore the sensitivities of other thermal properties, including thermal conductivity, emissivity, absorption coefficient, density, and gas transport coefficient toward uncertainties. The third part of the analysis explores how sensitivity results differ between the pyrolysis model developed by milligram-scale experiments and bench-scale experiments.

The modeling results are presented by processing and analyzing the simulated HRR data. The simulated MLR results are not listed here due to length limits, but note that the MLR data were always in the same change pattern as with HRR.[10] HRR is obtained by multiplying the mass fluxes of individual gaseous components through the front surface and the corresponding heats of complete combustion (h_c) of gaseous decomposition products measured using MCC[11] and adding these contributions together. The ignition was assumed to occur as soon as a measurable number of flammable gases were released.[10]

Detailed information of the initial and adjusted properties used for simulation is given in Table 4. The key parameters include the activation energy (RE), pre-exponential factor (RA), and heat of reaction (RH) of 15 reactions and the density (CP), thermal conductivity (CT), emissivity coefficient (CE), and absorption coefficient (CA) of 17 condensed-phase components. For example, density data is assigned with the code of CP1−CP17, where CP1 refers to the density of the first component listed in Table 3, that is, the density of PLA, and CP17 refers to the density of PLA_APP_MEL_Res. RE1 refers to the activation energy of the first reaction listed in Table 1, that is, the activation energy of PLA + NOCOMP → PLA_MELT + NOCOMP, and RE15 refers to the activation energy of the final reaction listed in Tables 1 and 2.

Table 4. Code of Adjusted Parameters and Simulation Cases for Sensitivity Analysis

parameter name	unit	case code	total number of cases
density	ρ (kg m^{-3})	CP1−CP17	136
emissivity coefficient	ε	CE1−CE17	102
absorption coefficient	κ (m^2 kg^{-1})	CA1−CA17	88
thermal conductivity	k (W m^{-1} K^{-1})	CT1−CT17	140
activation energy	E (J mol^{-1})	RE1−RE15	120
pre-exponential factor	A (s^{-2})	RA1−RA15	120
heat of reaction	h (J kg^{-1})	RH1−RH15	120

For each code involving density, activation energy, pre-exponential factor, and heat of reaction, sensitivity analysis was performed to change the parameter from 80% of the original value listed in Tables 1−3 to 120% of the original value. For example, the original value of CP1 (density of PLA) was 1240 kg m^{-3}; sensitivity analysis was performed to change the value of CP1 to 80%, 85%, 90%, 95%, 105%, 110%, 115%, and 120% of the original value (model value), i.e., 992, 1054, 1116, 1178, 1302, 1364, 1426, and 1488 kg m^{-3}, respectively. Sensitivity analysis of activation energy (RE), pre-exponential factor (RA), and heat of reaction (RH) was performed by the same rule. For sensitivity analysis of emissivity and absorption coefficient (CE and CA), the physical significance must be considered. The fundamental idea was similar to the aforementioned methodology, that is, to change from 80% of the original value listed in Table 3 to 120% of the model value. However, additional rules were set such that the maximum absorption coefficient was limited to 1, and the maximum emissivity coefficient for residue components was limited to 100. In addition, with the exception of PLA, the thermal conductivity (CT) of other components is a function of temperature ($a + bT + cT^3$). Sensitivity analysis of CT was conducted by changing a, b, and c to 80%, 90%, 110%, and

https://doi.org/10.1021/acsomega.2c01402
ACS Omega 2022, 7, 19648−19664

Table 5. Summary of the Adjusted Parameters for Thermal Conductivity Sensitivity Analysis

component code	thermal conductivity ($a + bT + cT^3$)	analysis cases
CT1-1−CT1-8	0.12	80, 85, 90, 95, 105, 110, 115, 120% of the model value
CT2-1−CT2-8, CT3−CT9, CT13, CT14	$0.12 + 0.0005T$	a + 80%bT, a + 90%b, a + 110%bT, a + 120%bT, 80%a + bT, 90%a + bT, 110%a + bT, 120%a + bT
CT10-1−CT10-8, CT11-1−CT11-8	$0.3 + 0.002T$	a + 80%bT, a + 90%b, a + 110%bT, a + 120%bT, 80%a + bT, 90%a + bT, 110%a + bT, 120%a + bT
CT12-1−CT12-12	$0.03 + 0.0002T + 1 \times 10^{-9}T^3$	a + 80%bT + cT^3, a + 90%bT + cT^3, a + 110%bT + cT^3, a + 120%bT + cT^3, 80%a + bT + cT^3, 90%a + bT + cT^3, 110%a + bT + VT^3, 120%a + bT + cT^3, a + bT + 80%cT^3, a + bT + 90%cT^3, a + bT + 110%cT^3, a + bT + 120%cT^3
CT15-1−CT15-8	$0.5 + 0.0001T$	a + 80%bT, a + 90%b, a + 110%bT, a + 120%bT, 80%a + bT, 90%a + bT, 110%a + bT, 120%a + bT
A16T-1−CP17T-8, CP17T-1−CP17T-8	$0.06 + 5 \times 10^{-10}T^3$	80%a + cT^3, 90%a + cT^3, 110%a + cT^3, 120%a + cT^3, a + 80%cT^3, a + 90%cT^3, a + 110%cT^3, a + 120%cT^3

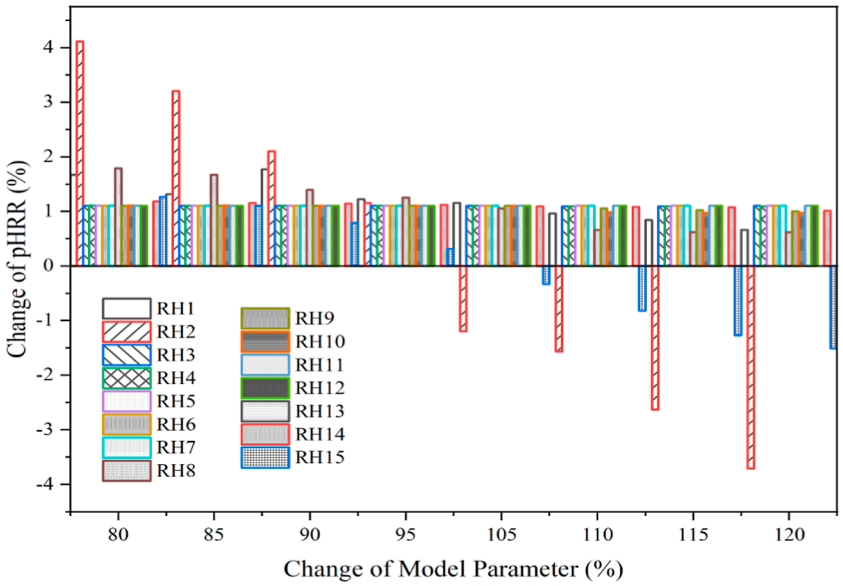

Figure 1. Summary of $\overline{\text{pHRR}}$ change rate for case RH.

120% of the model coefficient, respectively. Table 5 summarizes the adjusted parameters for thermal conductivity sensitivity analysis. Due to the different forms of thermal conductivity, the total analysis case amount of each component parameter or reaction parameter ranges from 8 to 12.

In summary, the entire sensitivity analysis project covers 826 cases, as summarized in Table 4. Sensitivity analysis compares the HRR profile before and after adjusting each parameter. The profile was quantitatively analyzed by four key indicators. The first indicator was set as $\overline{\text{pHRR}}$, corresponding to the average value of HRR from 0 to 180 s. This time was selected because, during this period, pure PLA exhibited significant mass loss and heat release.[10] The second indicator was set as the maximum HRR after 180 s (mHRR), indicating the position of the profile peak. The third indicator was set as the time to maximum HRR (tmHRR). The fourth indicator was set as the HRR values after 600 s (fHRR). The time of 600 s was set because according to the well-developed model, both HRR and MLR were reduced to zero (i.e., pyrolysis stopped) before 600 s. The final indicator was the total heat release during the entire pyrolysis (i.e., THR), which was calculated as the integration of HRR data with time. It should be noted that the purpose of these simulations was not to accurately predict the HRR but to provide a fundamental understanding of the impacts of model uncertainties on pyrolysis modeling results.

3. RESULTS AND DISCUSSION

3.1. Sensitivity Analysis of Reaction-Related Parameters. *3.1.1. Sensitivity of Heat of Reaction.* The heat of decomposition refers to the endothermic process from the condensed phase to the gas phase for polymers. The heat of decomposition is somewhat analogous to the latent heat of vaporization of a liquid, but a polymer must first break down into small and volatile products before vaporization.[13] The heat of decomposition sensitivity was analyzed by changing the heat of decomposition of each reaction into different values one by one, while the other input parameters of the model were unchanged. It should be mentioned that the heat of reaction in the pyrolysis model was assumed to be positive when the reaction is endothermic. However, when talking about the increase or decrease of heat of reaction in this paper, it refers to the absolute value.

Through calculation of 120 cases regarding the heat of reaction (RH1−RH15) of the composite material, it was found that with the value changing from 80% to 120% of the original model value, most of the reactions did not have a significant change. The change rate of $\overline{\text{pHRR}}$ for all cases is summarized in Figure 1. The most sensitive reaction is RH2. When the heat of reaction of R2 was reduced to 80% of the model value, the $\overline{\text{pHRR}}$ was improved by 4.11%. While with 120% change of heat of reaction of RH2, $\overline{\text{pHRR}}$ was reduced by 3.71%. The

https://doi.org/10.1021/acsomega.2c01402
ACS Omega 2022, 7, 19648−19664

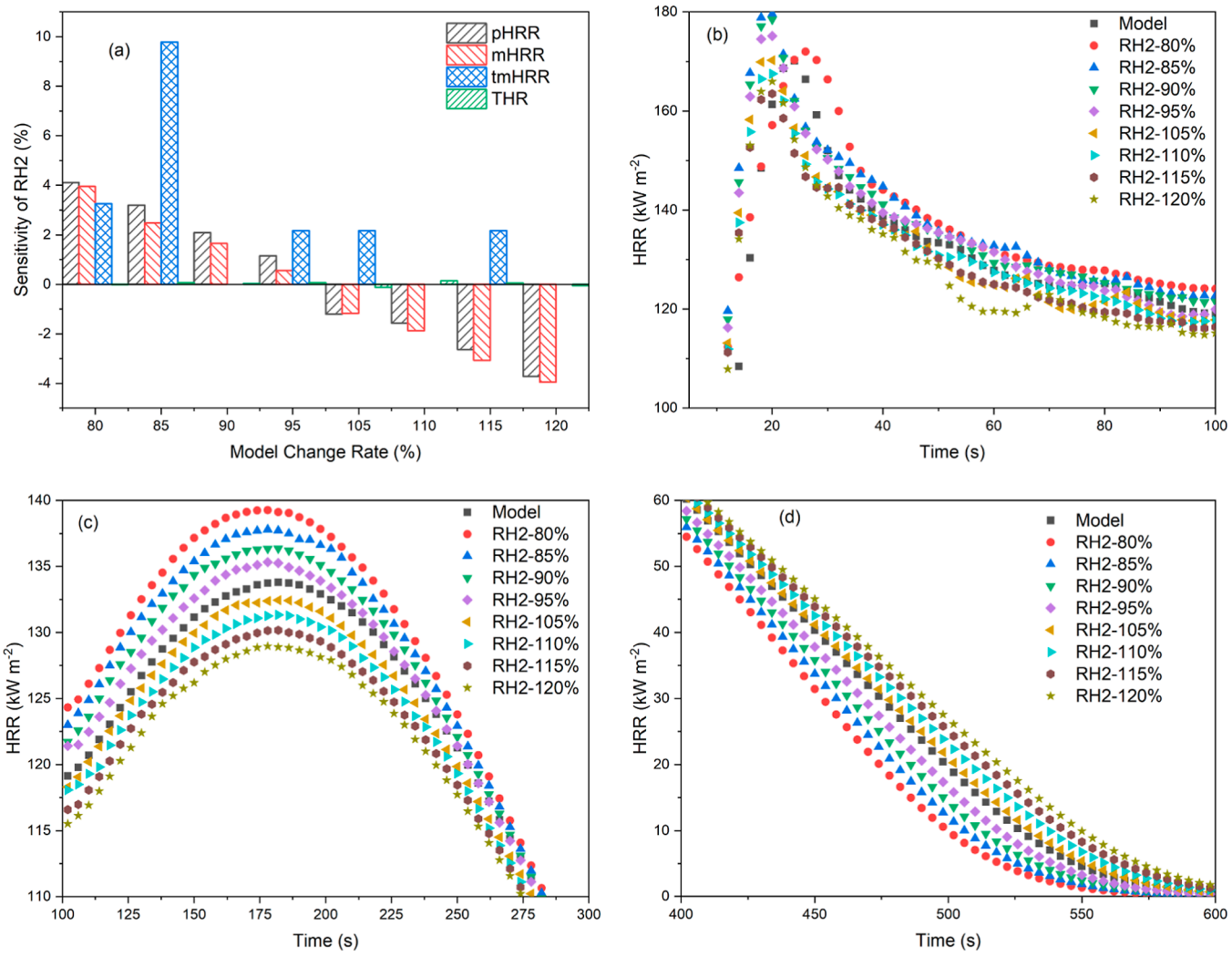

Figure 2. Overview of (a) indicator sensitivity and (b−d) HRR profiles of case RH2.

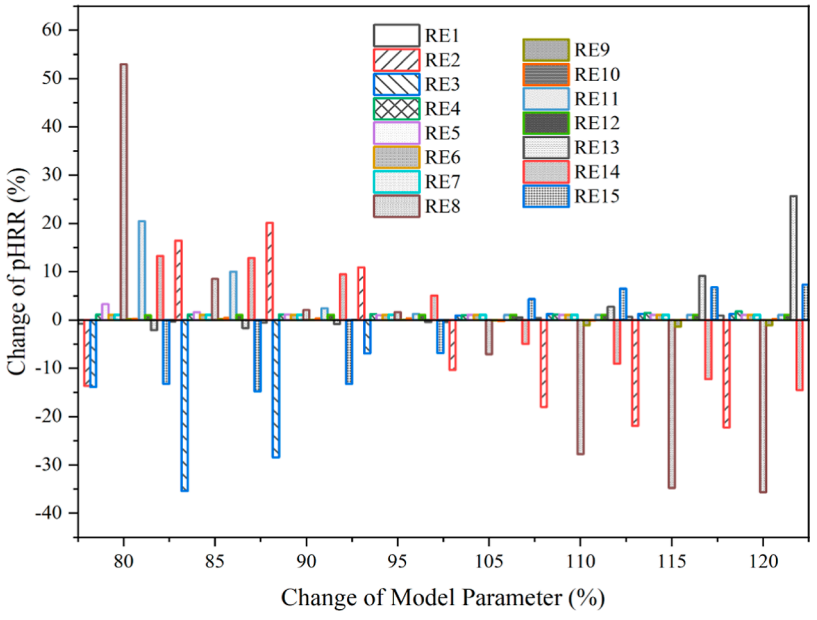

Figure 3. Summary of $\overline{\text{pHRR}}$ change rate for case RE.

https://doi.org/10.1021/acsomega.2c01402
ACS Omega 2022, 7, 19648−19664

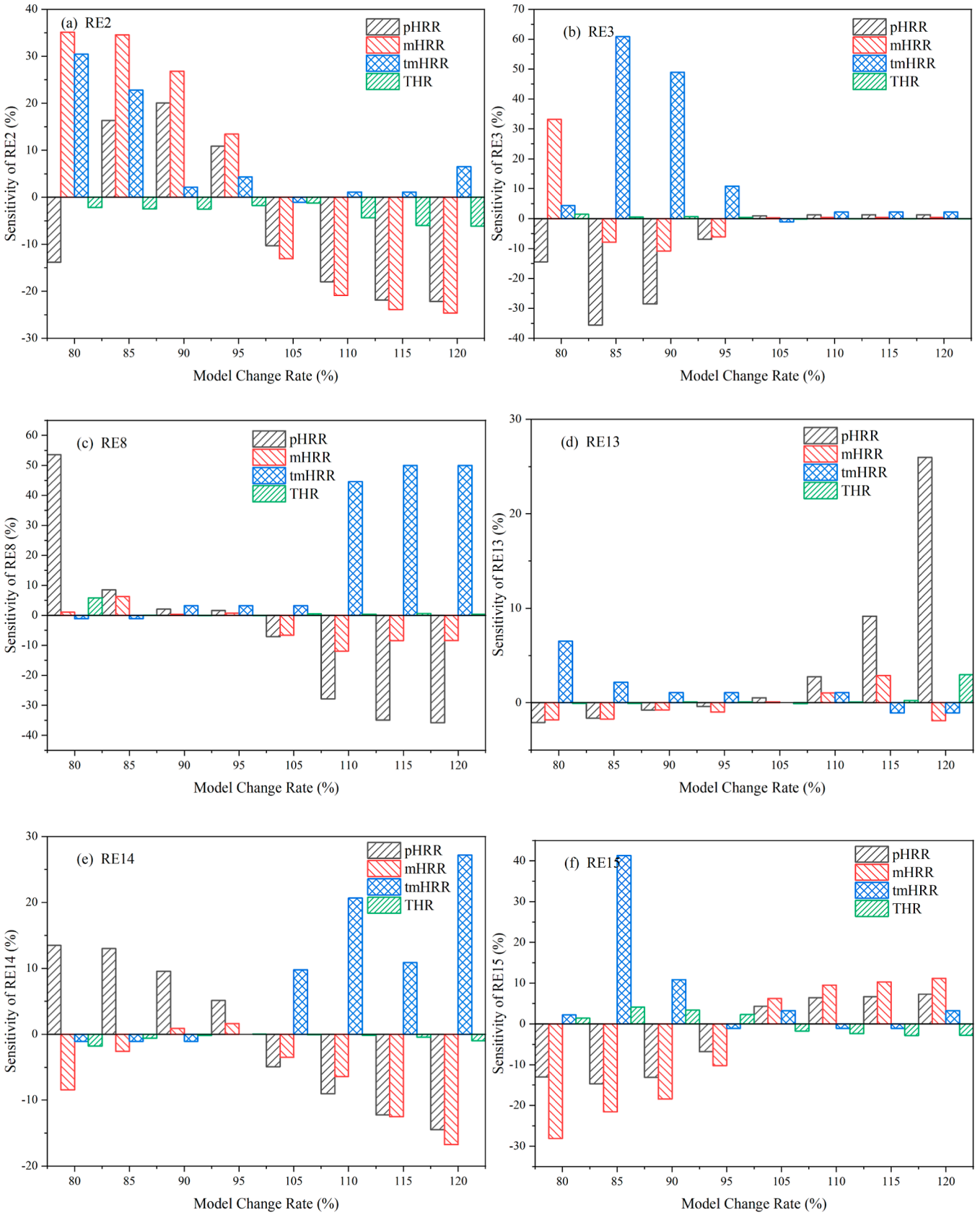

Figure 4. Overview of indicator sensitivity of case (a) RE2, (b) RE3, (c) RE8, (d) RE13, (e) RE14, and (f) RE15.

sensitivity was mainly due to the change of $\overline{\text{pHRR}}$, mHRR, and tmHRR, and yet, THR was changed less than 0.15%. The change rates of two key indicators for RH2 are presented by bar charts as shown in Figure 2a. The corresponding HRR profiles of RH2 are summarized in Figure 2b−d with dots.

https://doi.org/10.1021/acsomega.2c01402
ACS Omega 2022, 7, 19648−19664

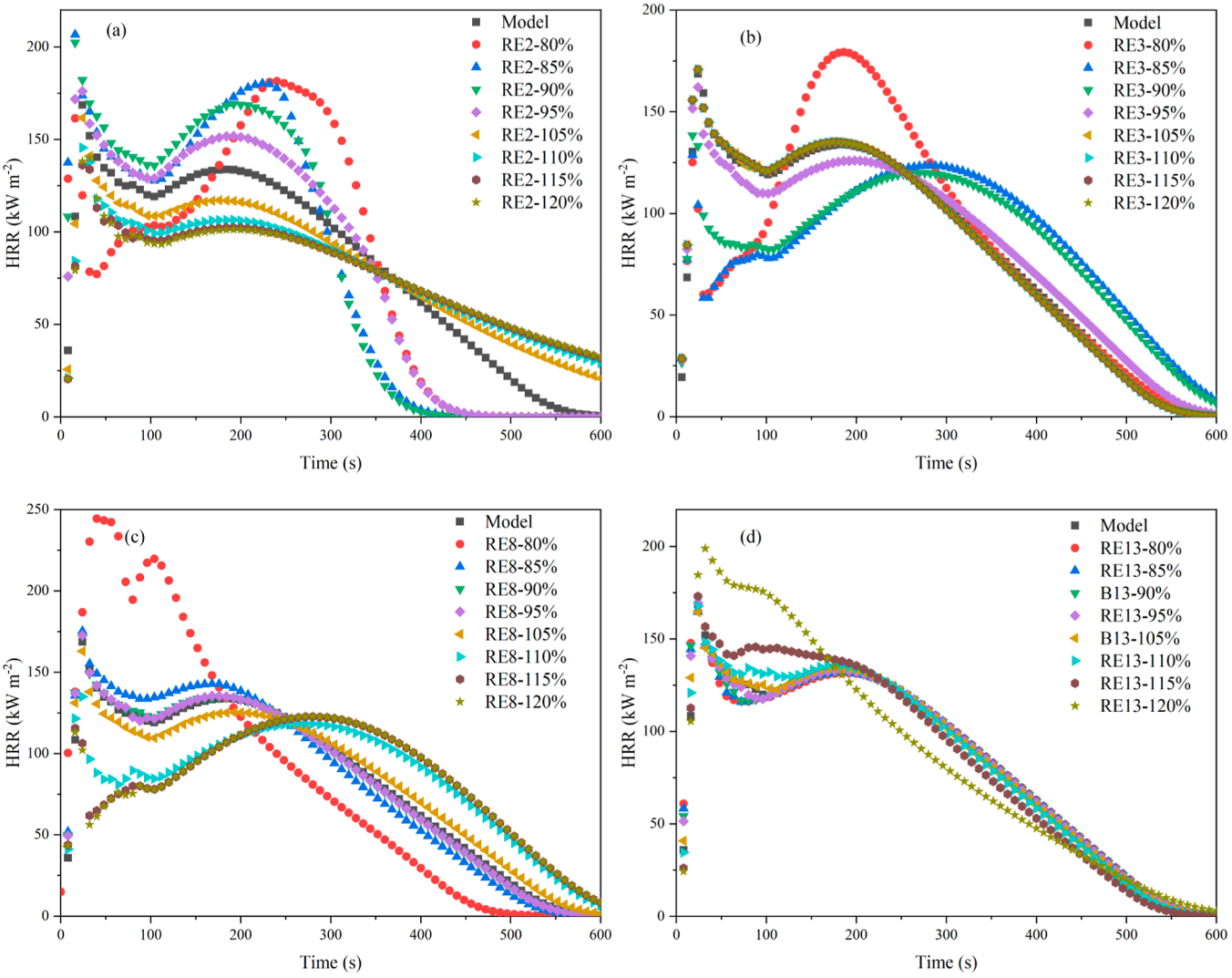

Figure 5. Overview of HRR profiles of case (a) RE2, (b) RE3, (c) RE8, (d) RE13, (e) RE14, and (f) RE15.

It can be seen from Figure 2a that, when increasing the heat of reaction of RH2, the change rate of both $\overline{\text{pHRR}}$ and mHRR became more significant. The positive and negative change rate was roughly in a symmetric distribution. In the initial pyrolysis stages, the HRR profiles were generally overlapped with each other, indicating that the parameter change did not influence the early decomposition stage. Before it reached $\overline{\text{pHRR}}$, the profiles from the highest to the lowest were in the order of 80% to 120%. Reducing the heat of reaction of RH2 would cause larger $\overline{\text{pHRR}}$ according to Figure 2c, but it also accelerated the pyrolysis process as the case with 80% change reached 0 by the minimum pyrolysis time. For other cases, their HRR profiles were in very similar patterns, with variations of less than 2%. Therefore, it can be concluded that with the exception of RH2, adjusting the heat of reaction in the model from 80% to 120% usually caused a change of less than 2% in the predicted fire behavior of the material. This is because the increase of heat of decomposition refers to the requirement of more heat to continue the pyrolysis and thus resulting in a slower pyrolysis rate.

3.1.2. Sensitivity of Activation Energy. For sensitivity of activation energy (RE1−RE15), results of indicators showed that the six reactions including RE2, RE3, RE8, and RE13−RE15 had significant differences in HRR profiles, if changing the original activation energy value from 80% to 120%. The change rate of $\overline{\text{pHRR}}$ for all cases is summarized in Figure 3. The corresponding results of six key reactions are summarized in Figures 4 and 5. Adjusting the activation energy of other reactions from 80% of the model value to 120% will contribute to pyrolysis model differences by less than 2%, which can be ignored and are not listed in the paper.

Sensitivity of selected six reactions showed different patterns. For case RE2, it mainly influenced mHRR and tmHRR, followed by $\overline{\text{pHRR}}$. RE2 corresponds to the decomposition of the melted PLA component. When increasing the activation energy of this reaction from 80% of the model value to 120%, the HRR profile moved toward a lower HRR value at the same pyrolysis time. In the case of 80% change, both mHRR and tmHRR increased by over 30%; on the contrary, both reduced by over 20% in the case of 120% change. It can be seen from Figure 5a that in the case of 80%−95%, the pyrolysis was finished within 450 s, indicating that the combustion of material was highly accelerated. However, in the case of 105%−120%, the pyrolysis process was largely delayed and less significant, requiring much longer time to be fully pyrolyzed. The phenomenon can be understood by the chemical meaning

https://doi.org/10.1021/acsomega.2c01402
ACS Omega 2022, 7, 19648−19664

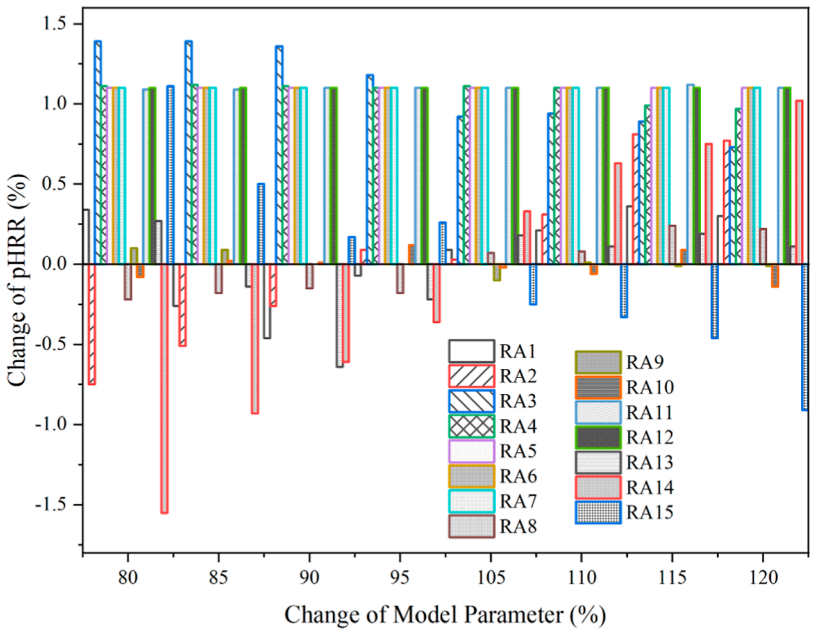

Figure 6. Summary of $\overline{\text{pHRR}}$ change rate for case RA.

of activation energy as the minimum amount of energy that is required to activate atoms or molecules to a condition in which they can undergo chemical transformation.[20] It should be noted that the change rate of THR was less than 5% for all cases, so the change of model parameters could influence the pyrolysis rates and yet did not control the total heat released by combustion of materials.

RE3 refers to the decomposition of MEL into residue and gases. Relevant results are summarized in Figures 4b and 5b. Reducing the activation of this reaction from 80% to 95% of the model value had a significant effect on the pyrolysis process, particularly in the case of 80%. It could even change the reaction mechanism as the profile evolution pattern was highly changed. Therefore, if the input activation energy of R2 in pyrolysis modeling was set to be lower than the original model value, it may cause significant differences in fire behavior prediction. However, if the input parameter was 120% higher than the original value, it would have very limited influence on the predicted results.

The sensitivity and HRR profile of RE8 are presented in Figures 4c and 5c, respectively. Apparently, reducing the activation energy of this reaction from 85% to 95% had a limited effect on the pyrolysis process. However, with reduction to 80%, the profile was highly changed and cannot reflect the pyrolysis process anymore. If the input parameter was increased from 105% to 120% of the model value, it would have an obvious influence on the predicted HRRs, particularly in terms of tmHRR. If the input activation energy of R8 in pyrolysis modeling was set to be higher than the original model value, it may cause delays in capturing the critical pyrolysis behavior and thus underestimate the fire hazards of materials.

For cases of RE2 and RE8, changing the parameter to 80% of the model value would cause a major difference in the pyrolysis process, while for RE13, changing the model value to 115% or 120% had the most significant effect on prediction results. When the input activation energy of R13 was less than 115% of the original model value, it had a limited effect on prediction results. Relevant results are summarized in Figures 4d and 5d.

RE14 refers to the reactions of APP_MEL_Res1 to the final residue. The change tendency showed a symmetry pattern. By changing the activation energy of R14 from low (80% of the model value) to high (less than 100% of the model value), the $\overline{\text{pHRR}}$ change rate roughly reduced from 13% to 4%, but all the predicted $\overline{\text{pHRR}}$ was higher than the model result. On the contrary, by changing the activation energy of R14 from 105% of the model value to 120%, the $\overline{\text{pHRR}}$ change rate roughly increased from 4% to 17%, but all predicted $\overline{\text{pHRR}}$ was lower than the model result. During pyrolysis modeling, when the input activation energy of R14 was lower than the model value, it would overestimate the initial pyrolysis process with higher heat release and overestimate the pyrolysis time. On the other hand, if the input value of R14 was higher than the model value, it would underestimate both the initial pyrolysis behavior and the total pyrolysis time. Although the total heat release would not be of notable change, the pyrolysis rate would be much different. This would finally influence the decision making of fire fighters and material designers in relevant fields.

The sensitivity of RE15 was similar to that of RE14, but the positive and negative effect was inversed. Relevant results are summarized in Figures 4f and 5f, respectively. Lower activation energy led to lower $\overline{\text{pHRR}}$ and higher pyrolysis time. When the activation energy of R15 reduced to 80% of the model value, there was no obvious HRR peak any more. Then, with the increase of RE15, the predicted HRR profile gradually moved toward higher $\overline{\text{pHRR}}$, getting closer to the original model profile. If the input parameter was 105% of the model value and higher, the predicted HRR profile continually moved toward higher $\overline{\text{pHRR}}$, accelerating the pyrolysis process by reducing the total pyrolysis time. However, it was less significant for cases with the change rate of 105%−120%, compared to the cases with change rate of 80%−95%. Summarizing from cases of RE2, RE3, RE8, and RE13−RE15, for pyrolysis modeling of this composite material system, it is very necessary to use the most exact activation energy to predict the fire behavior of the material. The

https://doi.org/10.1021/acsomega.2c01402
ACS Omega 2022, 7, 19648−19664

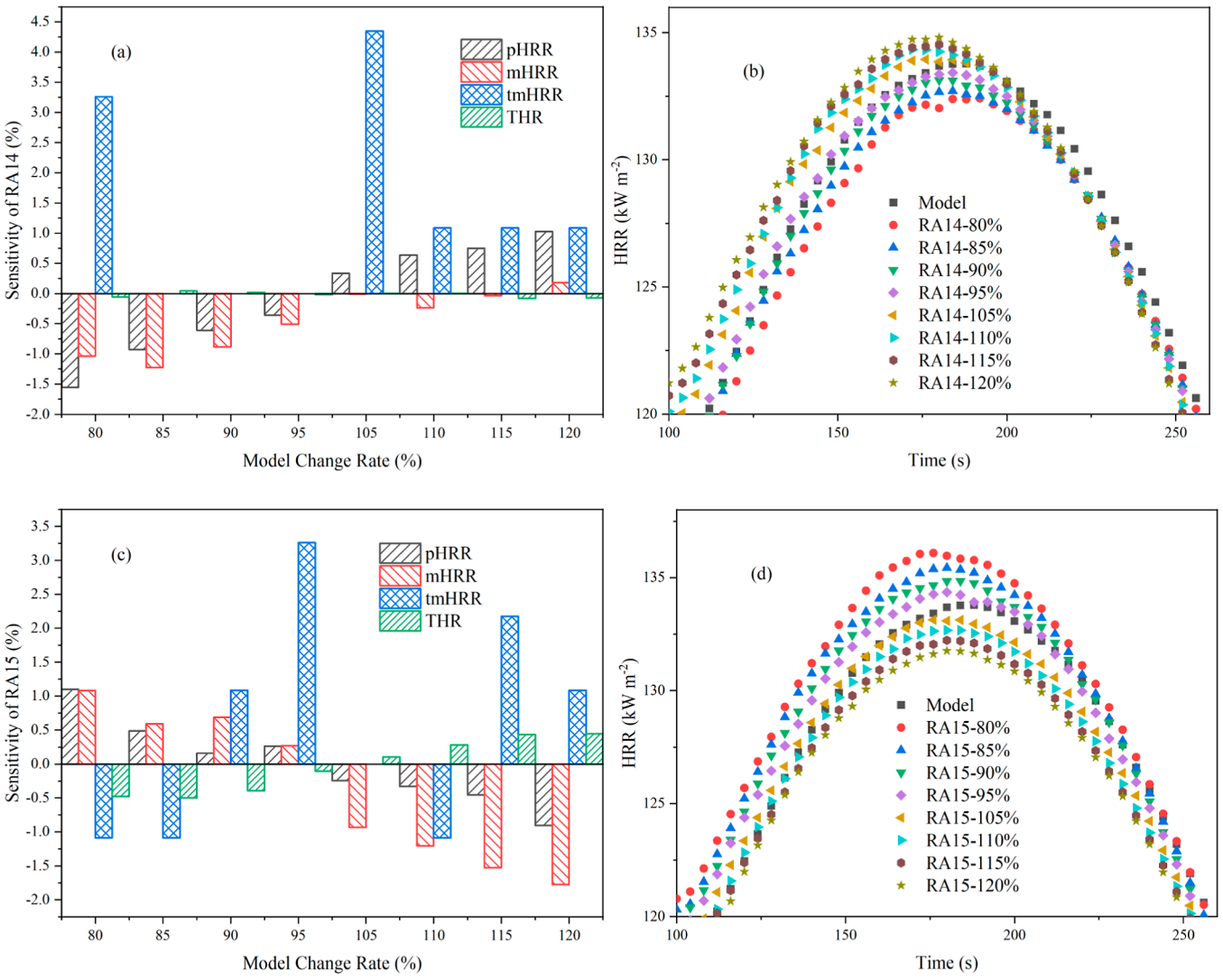

Figure 7. Overview of (a) indicator sensitivity and (b) HRR profiles of case RA14; (c) indicator sensitivity; and (d) HRR profiles of case RA15.

activation energy of intermediate reactions would cause significant sensitivity to the prediction results and thus influence the firefighting or composite material design decision-making process.

3.1.3. Sensitivity of Pre-exponential Factor. For sensitivity of pre-exponential factor (RA1−RA17), a summary of the $\overline{\text{pHRR}}$ change rate is presented in the indicator of HRR in Figure 6. The sensitivity of all cases is less than 2%. Therefore, adjusting the model value of pre-exponential factor from 80% to 120% would have limited effect on the predicted fire behaviors and thus can be ignored. In this study, two cases including RA14 and RA15 are selected for detailed analysis, as they were relatively more sensitive compared to other cases. Corresponding results are summarized in Figure 7.

It can be seen from Figure 7 that the effects of parameter on HRR profile were in an opposite pattern between RA14 and RA15. For RA14, reducing the pre-exponential factor would lead to higher $\overline{\text{pHRR}}$ and mHRR; reducing the pre-exponential factor increased both $\overline{\text{pHRR}}$ and mHRR. However, the change rate of both $\overline{\text{pHRR}}$ and mHRR was less than 2%. Although tmHRR was changed by over 2% in some cases, the total heat release was similar to each other. In summary, the input value of the pre-exponential factor for the composite material from 80 to 120% of the model value had no significant effect on the predicted fire behavior.

3.2. Sensitivity Analysis of Component-Related Parameters. *3.2.1. Sensitivity of Density.* The effects of density on the pyrolysis of the material were studied by only changing density value of the component one by one, while other input parameters remained the same. The virgin components refer to the raw materials functioning as initial reactants, that is, PLA, APP, and MEL. PLA_Melt, as a physical product by the melting of PLA, was also regarded as a virgin component in this study. For density sensitivity from CP1 to CP17, a summary of the change rate of $\overline{\text{pHRR}}$ is presented in Figure 8. The sensitivity in terms of $\overline{\text{pHRR}}$ was generally less than 5%, except the case of CP1 and CP15, that is, the density of PLA and APP_MEL_Res1, respectively. The detailed results of the two cases are summarized in Figure 9.

Clearly, the virgin materials with a lower density value required less time to start pyrolysis. Accordingly, the time to reach the peak HRR of the virgin material with a lower density was earlier than that of higher density materials. The peak HRR increased gradually with the rise of density value. This can be explained by the formula that relates thermal diffusivity (α) to energy transport and energy gradient. In eq 8, it can be

https://doi.org/10.1021/acsomega.2c01402
ACS Omega 2022, 7, 19648−19664

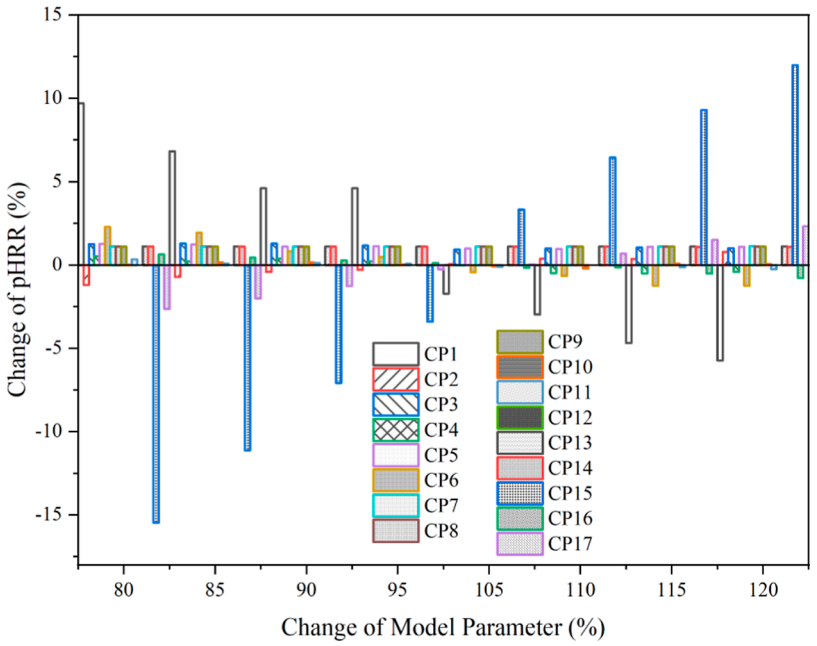

Figure 8. Summary of $\overline{\text{pHRR}}$ change rate for case CP.

observed that the thermal diffusivity will increase when only the density value is reduced, and thus, the energy gradient for a constant energy (q'') will also decrease.[13] It is more difficult for virgin materials with higher density value to easily transfer heat from the surface to underlying materials, and thus, more energy will be stored at the surface, resulting in more gas products and higher peak value of HRR. Since the mass concentration of PLA is nearly three times larger than that of APP, the effects of PLA density change on pyrolysis are more obviously observed.

$$q'' = \alpha \frac{\mathrm{d}}{\mathrm{d}x}(\rho c_p T) \tag{8}$$

For sensitivity of virgins, reducing the input density of PLA would cause higher $\overline{\text{pHRR}}$ and mHRR and shorter pyrolysis time. With parameter changes from 80% to 120%, the sensitivity in terms of both $\overline{\text{pHRR}}$ and mHRR was over 5%, whether it was increased or reduced. Besides, the total heat release showed significant sensitivity, with the absolute change rate higher than 5%. When reducing the PLA density from 120% of the model value to 80%, THR was reduced by nearly 33%. It should be mentioned that, when reducing the density of PLA, it did not influence the HRR before 50 s. In addition, with the increase of time, the effects of density reduction on the pyrolysis process acceleration became more obvious. It took less than half time for the material to finish the pyrolysis process if the density was reduced from 120% of the model value to 80%. Due to the limited amount of MEL in the composite, changing the density value of MEL or APP did not obviously influence the predicted HRR.

Different from the reaction parameters or component parameters that were obtained through inverse analysis of experiments, the density of PLA was a constant and did not require inverse modeling to determine, and thus, it is less likely to input the wrong value during fire behavior modeling. In other words, density of PLA can be known from the material provider. However, the sensitivity results indicate that the density of virgin materials would highly influence the predicted thermal stability of the composite system.

Although the pyrolysis model assumed 14 intermediate components in the condensed phase by inverse analysis of pyrolysis experiments, their density values may not be that sensitive. For the PLA/MEL/APP composite system, the simulation results of this paper indicated that only CP15 presented significant sensitivity. When CP15 was changed from 80% of the model value to 95%, it overestimated the pyrolysis process by increasing both $\overline{\text{pHRR}}$ and mHRR by over 5% and reducing THR by 5%−17%. On the contrary, when the value was changed from 105% of the model value to 120%, it would underestimate the pyrolysis process with lower $\overline{\text{pHRR}}$, lower mHRR, higher THR, and longer pyrolysis time. Therefore, the thermal stability and fire behavior of this composite is largely determined by the density of APP_MEL_Res1, which was generated from the chemical reactions between the two flame-retardant additives, APP and MEL.

3.2.2. Sensitivity of Thermal Conductivity. Thermal conductivity is a very important parameter to control the heat release of solids in different pyrolysis stages.[17,21] The effects of thermal conductivity on the pyrolysis of the composite material were studied with two perspectives, the virgin components and the residue components. For the virgin components, the thermal conductivity of PLA, APP, MEL, and PLA_Melt was respectively adjusted, with other input parameters being untouched. The thermal conductivity of PLA was proved to have insignificant effects on HRR since it did not directly participate in the pyrolysis process. Changing the thermal conductivity of APP or MEL also did not significantly influence the HRR, probably due to the limited amount in the composite system. Although the thermal conductivity value of PLA_Melt influenced the HRR from 100 to 250 s, the calculated integration of HRR was nearly the same despite the thermal conductivity change of PLA_Melt.

A summary of the thermal conductivity sensitivity in terms of $\overline{\text{pHRR}}$ is presented by Figure 10. The major case that influenced pyrolysis in terms of thermal conductivity is CT15.

https://doi.org/10.1021/acsomega.2c01402
ACS Omega 2022, 7, 19648−19664

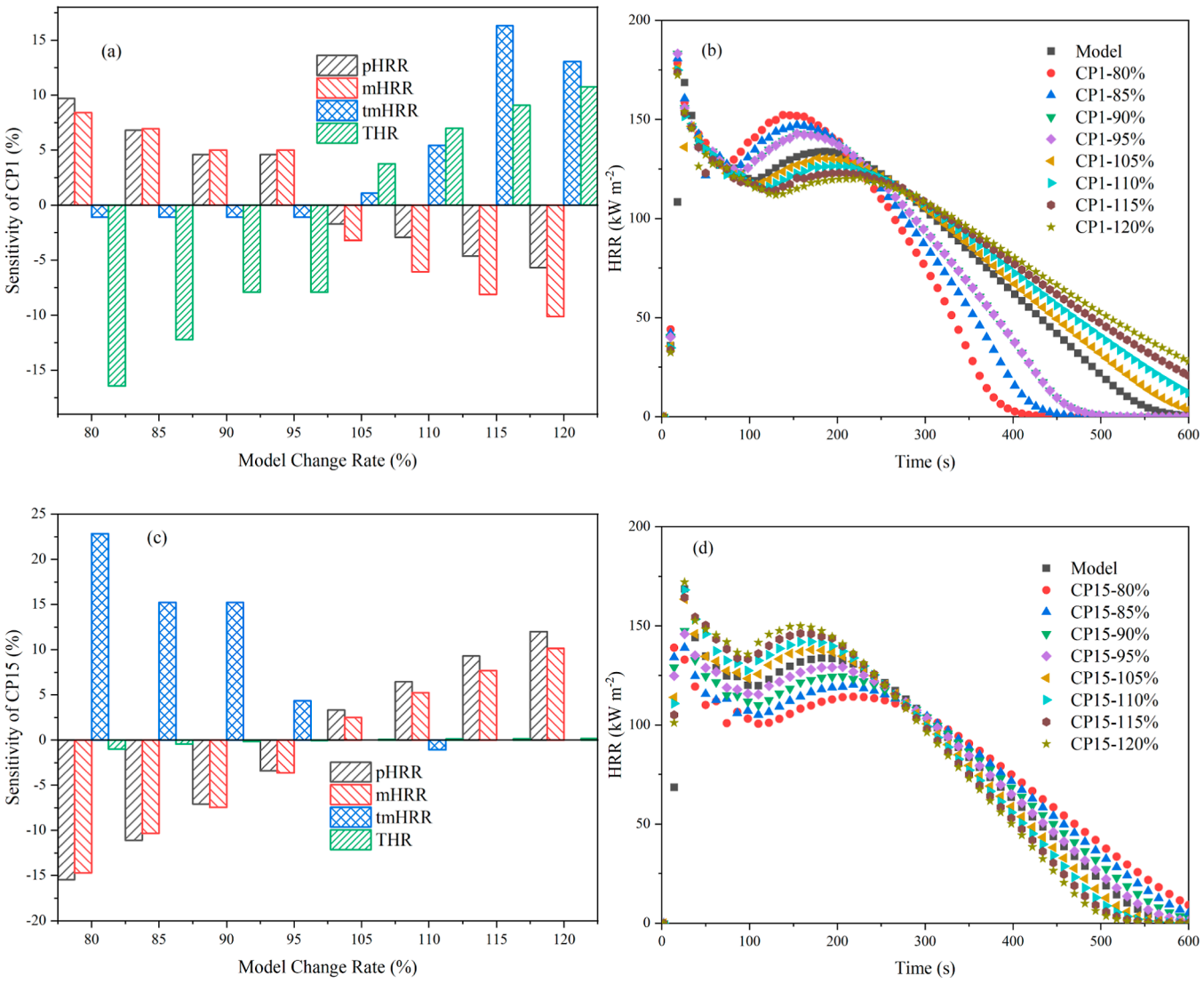

Figure 9. Overview of (a) indicator sensitivity and (b) HRR profiles of case CP1 and (c) indicator sensitivity and (d) HRR profiles of case CP15.

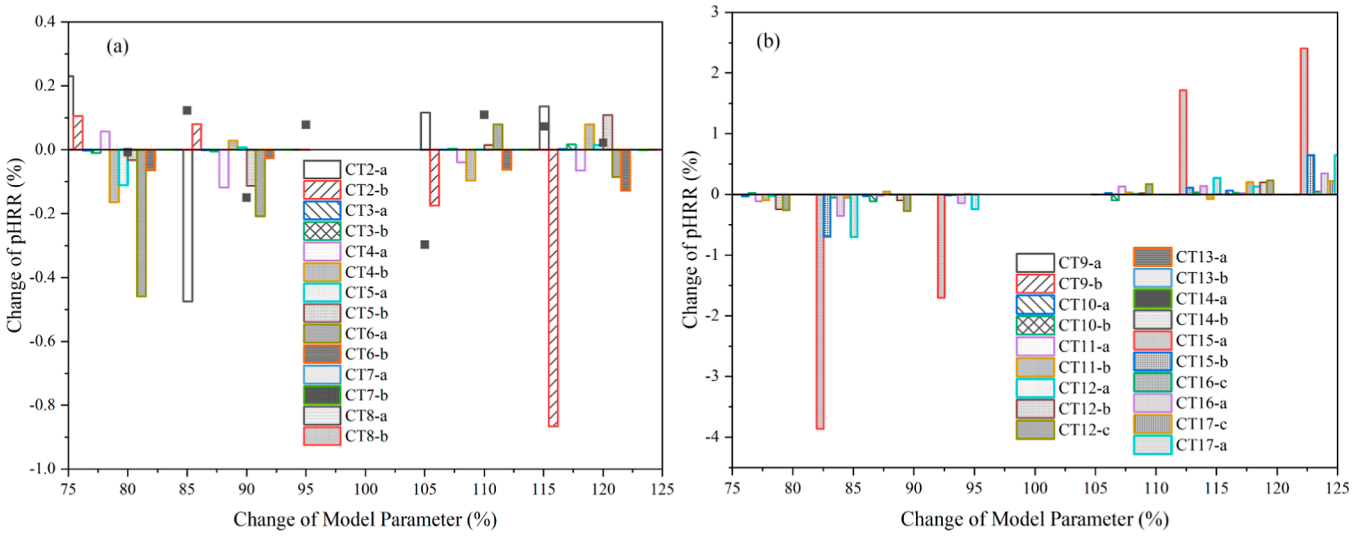

Figure 10. Summary of $\overline{\text{pHRR}}$ change rate for case CT with (a) CT2−CT8 and (b) CT9−CT17.

The thermal conductivity of C15 in the model was 0.5 + 0.0001T, in which 0.5 was set to be a and 0.0001 was set to be b for sensitivity analysis. From Figure 11b, the constant of CT15 (i.e., value of a) had the most significant sensitivity

https://doi.org/10.1021/acsomega.2c01402
ACS Omega 2022, 7, 19648−19664

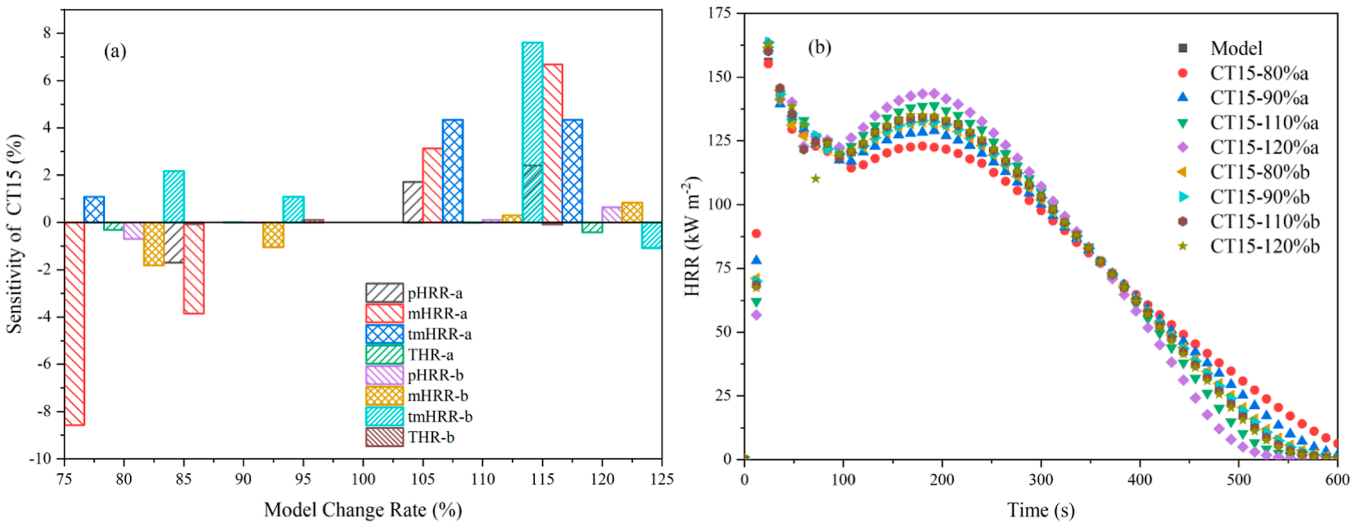

Figure 11. Overview of (a) indicator sensitivity and (b) HRR profiles of case CT15.

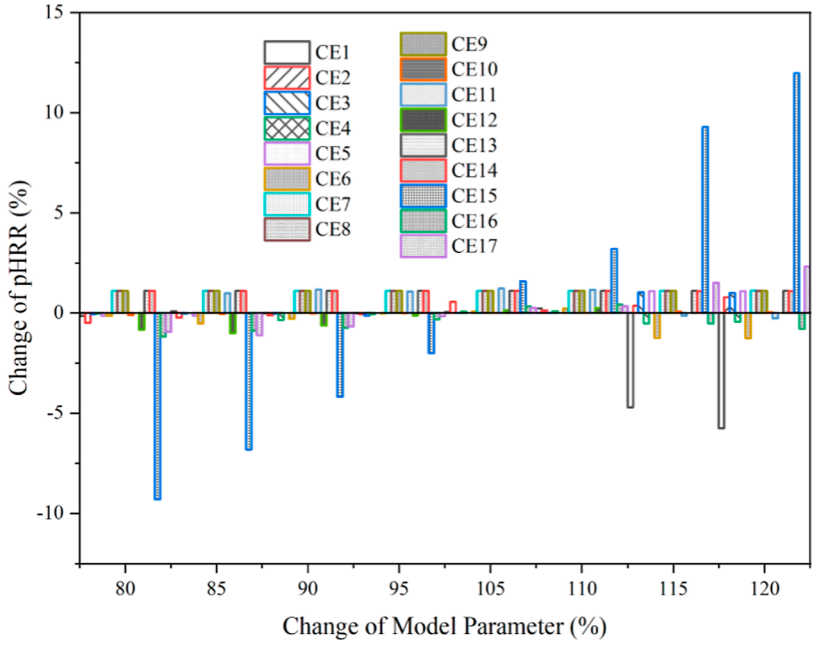

Figure 12. Summary of $\overline{\text{pHRR}}$ change rate for case CE.

among all cases. Reducing the value of *a* from 0.5 to 0.4, the $\overline{\text{pHRR}}$ would reduce by 3%, and the mHRR would reduce by 8%. Changing the value of *b* from 80% of the model value to 120% would also cause HRR differences, which was less significant compared to the sensitivity of *a*.

From Figure 11b, it can be seen that, in the pre-heating stage (before 50 s), the changes of thermal conductivity did not influence the HRR, probably because the char layer has not been formed or was of limited amount in this stage. The pyrolysis time for the simulated scenarios was the same (at least 50 s after the material was exposed to radiant flux). However, decreases in the peak of both MLR and HRR were identified with reduction of thermal conductivity. This is because when reducing the thermal conductivity of residual char formed at the material surface, the temperature gradient between the surface and inside of materials will be increased.[10] Therefore, it is more difficult for energy to be transferred into the materials. The indication for this phenomenon is that a more effective heat insulator can be formed by reducing the thermal conductivity value of the char layer. Accordingly, the materials inside will pyrolyze more slowly and the peak HRR will decrease.

3.2.3. Sensitivity of Emissivity and Absorption Coefficients. Sensitivity analysis of emissivity (CE1−CE17) and absorption coefficients (CA1−CA17) was conducted by changing the emissivity or absorption one by one from 80% of the model value to a higher value and keeping the other input parameters unchanged. Due to the physical significance of the two parameters, the adjustment was not from 80% to 120% with a 5% gradient anymore. As mentioned in Section 2.3, the maximum emissivity coefficient (CE) was limited to 1, and the maximum absorption coefficient (CA) for residue components was limited to 100.[10] No significant sensitivity in CA cases was found, which will be ignored in this paper due to length limits. A summary of the CE sensitivity in terms of $\overline{\text{pHRR}}$ is presented in Figure 12. It was generally less than 2%,

https://doi.org/10.1021/acsomega.2c01402
ACS Omega 2022, 7, 19648−19664

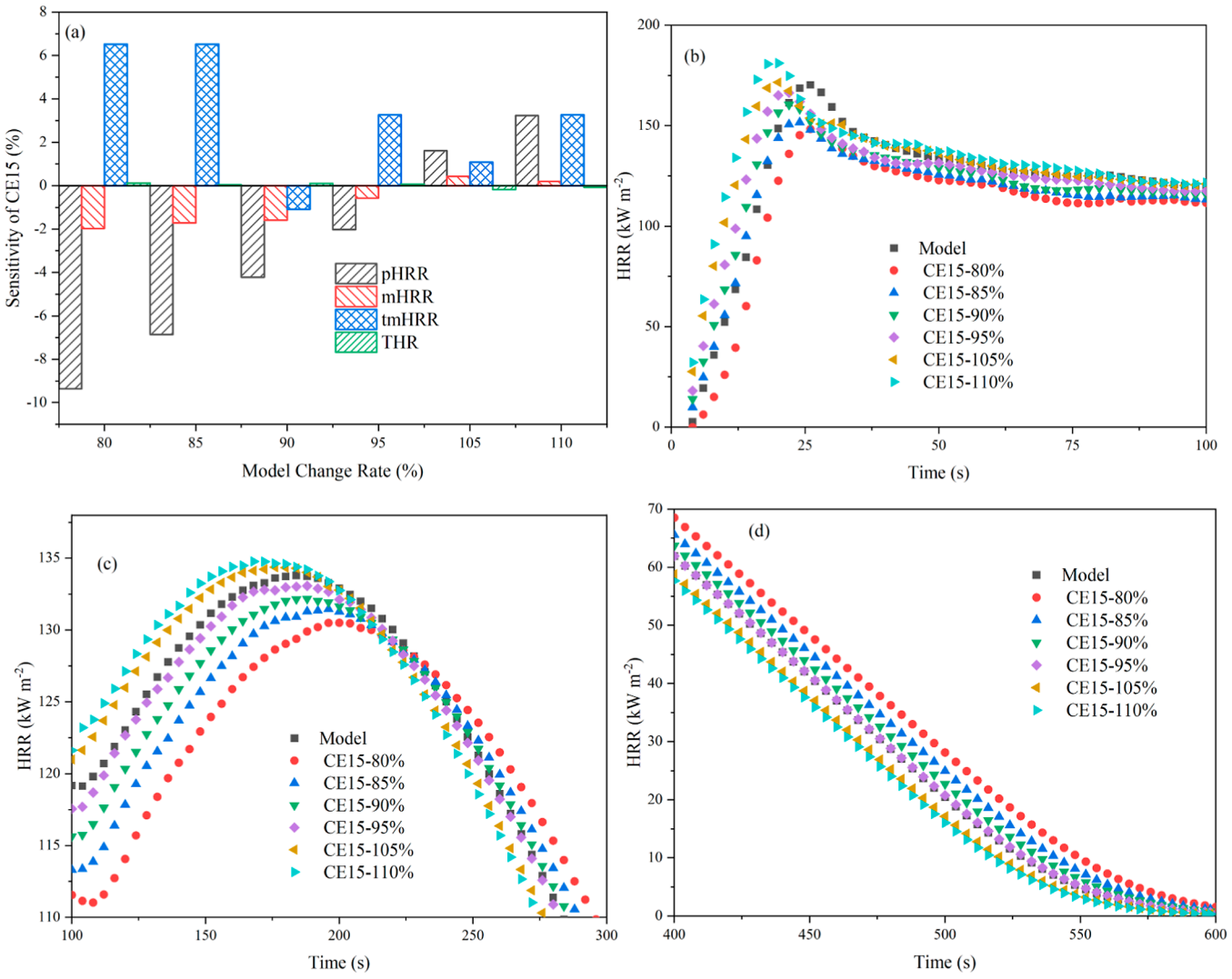

Figure 13. Overview of (a) indicator sensitivity and (b−d) HRR profiles of case RE2.

Component	CP	CE	CA	CT	Component	CP	CE	CA	CT
C1					C10				
C2					C11				
C3					C12				
C4					C13				
C5					C14				
C6					C15				
C7					C16				
C8					C17				
C9									

Reaction	RE	RA	RH	Reaction	RE	RA	RH
R1				R9			
R2				R10			
R3				R11			
R4				R12			
R5				R13			
R6				R14			
R7				R15			
R8							

CP-density; CE-emissivity; CA-absorption coefficient; CT-thermal conductivity; RE-activation energy; RA- pre-expotional factor; RH-heat of decomposition;

Grey:<2%; Blue:2%~5%; Green:5%~10%; Yellow:10%~15%; Red:>15%.

Figure 14. Summary of model sensitivity for 17 components and 15 reactions in terms of $\overline{\text{pHRR}}$ change rate for PLA70MEL5APP25 based on the bench-scale pyrolysis model. Note that the sensitivity results above are based on the pyrolysis model developed from inverse analysis of both bench-scale and milligram-scale experiments.[10,11] In the bench-scale experiments, the composite material with a certain thickness and diameter was exposed to radiation provided by a cone heater.[10] To conduct such inverse analysis, it requires to capture the MLR, thickness change, and back-surface temperature of the material at the same time. Therefore, this method requires complex experimental conditions and mathematical treatment. In some cases, researchers may only use milligram-scale experiments to capture input parameters for pyrolysis modeling. General milligram-scale experiments include TG, DSC, and MCC.[11] These techniques have been applied in an earlier work to develop the simplified pyrolysis model listed in Tables 1 and 2.

with the exception of CE15. The corresponding indicator sensitivity and HRR profiles are summarized in Figure 13. The changing pattern is obvious in Figure 13b−d. With the increase of CE15, both $\overline{\text{pHRR}}$ and mHRR increased as it accelerated

https://doi.org/10.1021/acsomega.2c01402
ACS Omega 2022, 7, 19648−19664

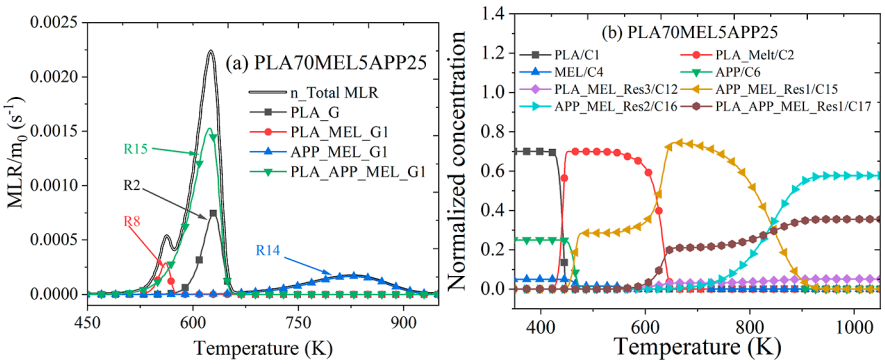

Figure 15. (a) Normalized MLR of each gaseous component from total MLR and (b) normalized concentration for each condensed-phase component by an initial sample mass for PLA70MEL5APP25 based on the milligram-scale pyrolysis model.

the entire pyrolysis process. There was no notable change in the total heat release. Changing the parameter of other components from 80% of the model value to the maximum did not cause primary changes in the predicted heat release profiles.

3.3. Effects of Experimental Scales on Pyrolysis Model Sensitivity. Summarizing the sensitivity results of reaction-related parameters in Section 3.1 and the sensitivity of component-related parameters in Section 3.2, it can be seen that among the 826 calculated cases, there were limited cases that showed significant sensitivity (with the change rate of $\overline{\text{pHRR}}$ being higher than 2%) when changing the parameter from 80% of the model value to 120% of the model value. Using different colors to present different levels of sensitivity, the sensitivity for 17 components and 15 reactions in terms of $\overline{\text{pHRR}}$ change rate for the composite material of PLA70MEL5APP25 is plotted in Figure 14. The blocks in gray indicate that the sensitivity is less than 2%. Accordingly, the blocks in blue, green, and red refer to a sensitivity of 2%−5%, 5%−10%, and higher than 15%, respectively. Note that the two plots only summarize the change rate of $\overline{\text{pHRR}}$, as it can reflect the thermal stability of the material once exposed to fire.

Generally, although there are 17 components and 15 reactions in the developed bench-scale pyrolysis model, the input parameters of only seven reaction-related parameters (R2, R3, R5, R8, R13, R14, and R15) and five component-related parameters (C1, C6, C12, C15, and C17) had primary effects on the predicted fire behavior in terms of HRR. R2 refers to the pyrolysis of melted PLA. This is because in the composite material, the primary thermal behavior is attributed to the thermal decomposition of PLA. R3 is the first step in the pyrolysis of MEL. R5 is the first step in the pyrolysis of APP. R8 is the reaction between melted PLA and MEL. R13 is the reaction between APP and MEL, which generates a new condensed-phase component (i.e., APP_MEL_Res1). R14 relates to the further decomposition of part of APP_MEL_Res1. The other part of APP_MEL_Res1 reacts with melted PLA to produce some final residue (chars), corresponding to R15. Therefore, the pyrolysis modeling results are highly related to the kinetics of reactions between virgin components or reactions where the virgin components played a significant role in. Among the three kinds of reaction-related parameters, the activation energy is much more sensitive than the heat of reaction or pre-exponential factor.

The five sensitive condensed-phase components include C1 (PLA), C6 (APP), C12 (PLA_MEL_Res3), C15 (APP_MEL_Res1), and C17 (PLA_APP_MEL_Res1). Two of them are virgin components. The sensitivity of MEL-related properties could be ignored because the simulated composite material only consists of 5 wt % MEL. Consistent with the sensitivity of reaction-related parameters, components generated from reactions between virgin components or reactions where virgin components played role in are generally of higher significance in pyrolysis modeling. Among the four types of component-related parameters, inputting the proper density is generally important for the prediction of fire behavior of the material. These sensitivity results provide clear information about how each condensed-phase component and reaction influence the pyrolysis behavior at different temperatures and thus simplify the pyrolysis modeling, fire behavior prediction, and design of new composite materials.

To explore how experiment scale could influence the sensitivity of the developed pyrolysis models, a series of processing of milligram-scale modeling data of PLA70MEL5APP25 was conducted by separating the MLR of each gaseous component from the total MLR data and isolating the concentration of each component from the entire concentration (which was set to be 1). The processed results with the corresponding temperature regions are given in Figure 15. It only presented major components that played a role in mass loss or concentration change. The major condensed-phase components were selected according to the initial-mass-normalized MLR (less than 0.0001 s^{-1} in all temperature regions); the major gaseous components were defined as gases with normalized concentration lower than 0.01 in all temperature regions. The other components were not shown in the figure due to their insignificant impacts.

From Figure 15a, it can be seen that the MLR profile had a small peak before 580 K, followed by its major sharp peak from 580 to 680 K and a third wide peak from 680 to 1000 K. The production of PLA_MEL_G1 (generated by R8) contributed to the first small peak. PLA_APP_MEL_G1 (generated by R15) and PLA_G (generated by R2) contributed to the major mass loss at a temperature region of 500−675 K and 570−675 K, respectively. The third MLR peak was due to the generation and consumption of APP_MEL_G1 (generated by R14). In summary, the major reactions that could possibly influence the pyrolysis process of PLA70MEL5APP25 include reactions 2, 8, 14, and 15. The reactions related to virgin MEL, virgin APP, or the interactions between PLA and APP were of insignificant impacts on mass loss of the composite material.

From Figure 15b, it can be seen that the eight major condensed-phase components contributed to the consumption of the condensed phase of PLA70MEL5APP25, including

https://doi.org/10.1021/acsomega.2c01402
ACS Omega 2022, 7, 19648−19664

three virgin materials (PLA, MEL, and APP), C2 (PLA_Melt), C15 (APP_MEL_Res1), C12 (PLA_MEL_Res3), C16 (APP_MEL_Res2), and C17 (PLA_APP_MEL_Res1). The primary reactions and components presented in Figure 15 can to a large extent reflect the sensitivity of the pyrolysis model developed at the milligram scale. Finally, it can be concluded that sensitivity analysis of bench-scale pyrolysis model identified two additional primary reactions, including R3 and R5. R3 corresponds to the pyrolysis of MEL into the residue and gases in a stoichiometric ratio of 0.82:0.18, and R5 is the pyrolysis of APP into the residue and gases in a stoichiometric ratio of 0.9:0.1. The processing at milligram scale did not identify the two components, largely because the analysis was based on the mass loss behavior of the generated gaseous components, which in two reactions were of a very limited amount. Regarding the components, sensitivity analysis at milligram scale identified three new components that have high sensitivity, including a virgin (MEL), C2 (PLA_Melt), and C16 (APP_MEL_Res2). C2 played an important role in the early decomposition stage by R2, and C16 mainly influenced the pyrolysis behavior at a higher temperature region. Although these two components are significant in pyrolysis modeling at the milligram scale, their influence on the fire behavior of materials at the bench scale becomes less important and thus can be ignored. Therefore, the pyrolysis models developed at the milligram scale could be quite different from that obtained by inverse analysis of bench-scale experiments. These findings alert the composite material designers and fire modeling engineers to select the proper input model under relevant scenarios. Generally, it is better to conduct bench-scale experiments to develop pyrolysis models as milligram-scale experiments cannot reflect the heat and mass transfer inside the material with different thicknesses, and thus, the predicted fire behavior calculated by the milligram-scale model could be less reliable.

4. CONCLUSIONS

On the basis of a well-developed bench-scale pyrolysis model, this study explored the sensitivity of pyrolysis model on flammability of a composite material system of PLA blended with MEL and APP. Focusing on the material with a composition of 70 wt % PLA and 25 wt % APP, the sensitivity of both reaction-related parameters and condensed-phase component-related parameters regarding material's flammability prediction was explored by simulating HRR under a certain radiation condition. Each reaction-related or component-related parameter of a previously validated bench-scale pyrolysis model was adjusted from 80% to 120% with a 5% or 10% gradient to explore the sensitivity. By processing the HRR profiles of 826 simulation cases, it was found that the input parameters of only seven reaction-related parameters and five component-related parameters had primary effects on the predicted fire behavior in terms of HRR. The pyrolysis modeling results are highly related to the kinetics of reactions between virgin components or reactions where the virgin components played an important role in, including the pyrolysis of melted PLA, the first step in the pyrolysis of MEL, the first step in the pyrolysis of APP, the reaction between melted PLA and MEL, the reaction between APP and MEL, and further decomposition of the generated new condensed-phase component. Particularly, the activation energy of these reactions, with sensitivity larger than 5% or 15%, is much more sensitive than the heat of reaction or pre-exponential factor. The heat of decomposition of pyrolysis of melted PLA had a sensitivity ranging from 2% to 5%. The pre-exponential factor of all reactions had a sensitivity less than 2%, which can be ignored. Consistent with the sensitivity of reaction-related parameters, components generated from reactions between virgin components or reactions where virgin components played role in are significant in pyrolysis modeling. Particularly, inputting the proper density is generally important for the prediction of fire behavior as the density of these components showed sensitivity larger than 2%. These sensitivity results provide clear information about how each condensed-phase component and reaction influence the predicted pyrolysis behavior of the composite material at different temperatures and thus simplify the pyrolysis modeling, fire behavior prediction, and design of new composite materials.

AUTHOR INFORMATION

Corresponding Author

Qi Sun − *School of Civil and Environmental Engineering, Ningbo University, Ningbo, Zhejiang 315211, P.R. China*; orcid.org/0000-0002-6198-7836; Phone: +8615968907583; Email: skdsunqi@163.com, sunqi@nbu.edu.cn

Authors

Zeyue Shen − *School of Civil and Environmental Engineering, Ningbo University, Ningbo, Zhejiang 315211, P.R. China*

Yue Qiu − *School of Civil and Environmental Engineering, Ningbo University, Ningbo, Zhejiang 315211, P.R. China*

Weichen Song − *School of Civil and Environmental Engineering, Ningbo University, Ningbo, Zhejiang 315211, P.R. China*

Complete contact information is available at: https://pubs.acs.org/10.1021/acsomega.2c01402

Author Contributions

Z.S. involved in calculations, graphing, and writing. Yue Qiu involved in calculations. W.S. involved in graphing and conceptualization. Q.S. involved in conceptualization, methodology, writing, validation, and corresponding.

Funding

The General Scientific Research Project of Education Department of Zhejiang Province (#Y202146326). The Open Fund of Collaborative Innovation Center of Coastal Urban Rail Transit, Ningbo University (#432101753).

Notes

The authors declare no competing financial interest.

ACKNOWLEDGMENTS

The corresponding author Q.S. would like to thank Professor Stoliarov, Stanislav I. and Professor Yan Ding for their guidance of pyrolysis modeling for the composite material during her visit at the University of Maryland, College Park.

REFERENCES

(1) (a) Bal, N. Forty years of material flammability: An appraisal of its role, its experimental determination and its modelling. *Fire Saf. J.* **2018**, *96*, 46−58. (b) Steinhaus, T. Determination of intrinsic material flammability properties from material tests assisted by numerical modelling. BRE Thesis, The University of Edinburgh, 2010. (c) Yuen, A. C. Y.; Chen, T. B. Y.; Yeoh, G. H.; Yang, W.; Cheung, S. C.-P.; Cook, M.; Yu, B.; Chan, Q. N.; Yip, H. L. Establishing pyrolysis

https://doi.org/10.1021/acsomega.2c01402
ACS Omega 2022, 7, 19648−19664

kinetics for the modelling of the flammability and burning characteristics of solid combustible materials. *J. Fire Sci.* **2018**, *36*, 494−517.
(2) (a) Palanikumar, K.; Thiagarajan, R.; Latha, B. *Bio-Fiber Reinforced Composite Materials*; Springer, 2022. (b) Qin, D.; Sang, L.; Zhang, Z.; Lai, S.; Zhao, Y. Compression Performance and Deformation Behavior of 3D-Printed PLA-Based Lattice Structures. *Polymers* **2022**, *14*, 1062. (c) Srivastava, V.; Singh, S.; Das, D. Biodegradable Fibre-Based Composites as Alternative Materials for Sustainable Packaging Design. *Proceedings of the International Conference on Sustainable Design and Manufacturing*; Springer, 2021; pp 87−98. (d) Wang, Q.; Chen, W.; Zhu, W.; McClements, D. J.; Liu, X.; Liu, F. A review of multilayer and composite films and coatings for active biodegradable packaging. *NPJ Sci. Food* **2022**, *6*, 18.
(3) Ghorbani, Z.; Webster, R.; Lázaro, M.; Trouvé, A. Limitations in the predictive capability of pyrolysis models based on a calibrated semi-empirical approach. *Fire Saf. J.* **2013**, *61*, 274−288.
(4) Bal, N. Uncertainty and Complexity in Pyrolysis Modelling. BRE Thesis, The University of Edinburgh, 2012.
(5) (a) Ding, C.; Wang, D.-Y. Flame-Retardant Wood Plastic Composites. *Advances in the Toxicity of Construction and Building Materials*; Elsevier, 2022; pp 117−136. (b) Qiu, S.; Sun, J.; Li, H.; Gu, X.; Fei, B.; Zhang, S. A green way to simultaneously enhance the mechanical, flame retardant and anti-ultraviolet aging properties of polylactide composites by the incorporation of tannic acid derivatives. *Polym. Degrad. Stabil.* **2022**, *196*, 109831. (c) Zhou, S.-J.; Wang, H.-M.; Xiong, S.-J.; Sun, J.-M.; Wang, Y.-Y.; Yu, S.; Sun, Z.; Wen, J.-L.; Yuan, T.-Q. Technical Lignin Valorization in Biodegradable Polyester-Based Plastics (BPPs). *ACS Sustain. Chem. Eng.* **2021**, *9*, 12017−12042.
(6) (a) Ahmad, A.; Banat, F.; Alsafar, H.; Hasan, S. W. An overview of biodegradable poly (lactic acid) production from fermentative lactic acid for biomedical and bioplastic applications. *Biomass Convers. Biorefin.* **2022**, DOI: 10.1007/s13399-022-02581-3. (b) Maleki, H.; Azimi, B.; Ismaeilimoghadam, S.; Danti, S. Poly(lactic acid)-Based Electrospun Fibrous Structures for Biomedical Applications. *Appl. Sci.* **2022**, *12*, 3192. (c) More, N.; Avhad, M.; Utekar, S.; More, A. Polylactic acid (PLA) membrane—significance, synthesis, and applications: a review. *Polym. Bull.* **2022**. (d) Taib, N.-A. A. B.; Rahman, M. R.; Huda, D.; Kuok, K. K.; Hamdan, S.; Bakri, M. K. B.; Julaihi, M. R. M. B.; Khan, A. A review on poly lactic acid (PLA) as a biodegradable polymer. *Polym. Bull.* **2022**, *1*, 1−35.
(7) EL Messiry, M. Biodegradable Fibers, Polymers, Composites and Its Biodegradability, Processing and Testing Methods. *Bio-Fiber Reinforced Composite Materials* **2022**, 75−104.
(8) (a) Chen, Y.; He, J.; Sun, Z.; Xu, B.; Li, J.; Qian, L. Grafting Cellulose Nanocrystals With Phosphazene-containing Compound for Simultaneously Enhancing the Flame Retardancy and Mechanical Properties of Polylactic Acid. **2021**. (b) Wang, D.-Y.; Leuteritz, A.; Wang, Y.-Z.; Wagenknecht, U.; Heinrich, G. Preparation and burning behaviors of flame retarding biodegradable poly(lactic acid) nanocomposite based on zinc aluminum layered double hydroxide. *Polym. Degrad. Stabil.* **2010**, *95*, 2474−2480.
(9) (a) Fontaine, G.; Gallos, A.; Bourbigot, S. Role of montmorillonite for enhancing fire retardancy of intumescent PLA. *Fire Saf. Sci.* **2014**, *11*, 808−820. (b) Shabanian, M.; Kang, N.-J.; Wang, D.-Y.; Wagenknecht, U.; Heinrich, G. Synthesis of aromatic-aliphatic polyamide acting as adjuvant in polylactic acid (PLA)/ammonium polyphosphate (APP) system. *Polym. Degrad. Stabil.* **2013**, *98*, 1036−1042.
(10) Sun, Q.; Ding, Y.; Stoliarov, S. I.; Sun, J.; Fontaine, G.; Bourbigot, S. Development of a pyrolysis model for an intumescent flame retardant system: Poly(lactic acid) blended with melamine and ammonium polyphosphate. *Composites, Part B* **2020**, *194*, 108055.
(11) Ding, Y.; McKinnon, M. B.; Stoliarov, S. I.; Fontaine, G.; Bourbigot, S. Determination of kinetics and thermodynamics of thermal decomposition for polymers containing reactive flame retardants: Application to poly(lactic acid) blended with melamine and ammonium polyphosphate. *Polym. Degrad. Stabil.* **2016**, *129*, 347−362.
(12) (a) Chen, T. B. Y.; Liu, L.; Yuen, A. C. Y.; Chen, Q.; Yeoh, G. H. A multiphase approach for pyrolysis modelling of polymeric materials. *Exp. Comput. Multiph. Flow* **2021**, DOI: 10.1007/s42757-021-0122-3. (b) Li, J.; Gong, J.; Stoliarov, S. I. Gasification experiments for pyrolysis model parameterization and validation. *Int. J. Heat Mass Tran.* **2014**, *77*, 738−744. (c) Lautenberger, C. Gpyro3D: A Three Dimensional Generalized Pyrolysis Model. *Fire Safety Science-Proceedings of the Eleventh International Symposium*, 2014; p 193. (d) Ion, I. V.; Popescu, F.; Rolea, G. G. A biomass pyrolysis model for CFD application. *J. Therm. Anal. Calorim.* **2013**, *111*, 1811−1815.
(13) Zhang, F.; Cheng, Y.; Wang, W.; Sun, Y. Modeling the Effect of Thermophysical Properties on Pyrolysis of Intumescent Fire-retardant Materials. *J. Macromol. Sci., Part B: Phys.* **2013**, *52*, 1567−1577.
(14) Stoliarov, S.; Lyon, R. Thermo-kinetic model of burning for pyrolyzing materials. *Fire Saf. Sci.* **2008**, *9*, 1141−1152.
(15) Babrauskas, V.; Peacock, R. D. Heat release rate: the single most important variable in fire hazard. *Fire Saf. J.* **1992**, *18*, 255−272.
(16) (a) Mahmood, H.; Shakeel, A.; Abdullah, A.; Khan, M.; Moniruzzaman, M. A comparative study on suitability of model-free and model-fitting kinetic methods to non-isothermal degradation of lignocellulosic materials. *Polymers* **2021**, *13*, 2504. (b) Vinayak, A. *Mathematical Modeling & Simulation of Pyrolysis & Flame Spread in OpenFOAM*; Bergische Universität Wuppertal Wuppertal: Germany, 2017.
(17) Nyazika, T.; Jimenez, M.; Samyn, F.; Bourbigot, S. Pyrolysis modeling, sensitivity analysis, and optimization techniques for combustible materials: A review. *J. Fire Sci.* **2019**, *37*, 377−433.
(18) Swann, J. D.; Ding, Y.; Stoliarov, S. I. Characterization of pyrolysis and combustion of rigid poly(vinyl chloride) using two-dimensional modeling. *Int. J. Heat Mass Tran.* **2019**, *132*, 347−361.
(19) American Society for Testing and Materials. *Materials. Standard Test Method for Heat and Visible Smoke Release Rates for Materials and and Products Using an Oxygen Consumption Calorimeter*; ASTM International, 2016.
(20) Truhlar, D. G. Interpretation of the activation energy. *J. Chem. Educ.* **1978**, *55*, 309.
(21) Chaurasia, A.; Babu, B. Modeling & Simulation of Pyrolysis of Biomass: Effect of Thermal Conductivity, Reactor Temperature and Particle Size on Product Concentrations. *International Conference on Energy and Environmental Technologies for Sustainable Development (ICEET-2003)*: Citeseer, 2005; pp 8−10.

https://doi.org/10.1021/acsomega.2c01402
ACS Omega 2022, 7, 19648−19664